

THE FOURTH ASIAN CONGRESS OF FLUID MECHANICS

August 21-25, 1989 Hong Kong

Simulation of Unsteady Separated Flows

Kunio Kuwahara
The Institute of Space and Astronautical Science,
Yoshinodai, Sagami-hara, Kanagawa 229, Japan

Unsteady flows around a bluff body are simulated by solving the incompressible Navier-Stokes equations numerically. The mechanism of unsteady vortex shedding is studied by analysing the computed patterns of flow separation extensively.

Recent development of supercomputers has enabled to compute flow field using the grid system with the order of $100 \times 200 \times 300$ points; this number of grid points may not be sufficient to analyse a turbulent boundary layer but is good for laminar boundary layer.

Method of Computation

In this paper, we study unsteady boundary layer separation and vortex shedding around a bluff body by computation. The unsteady incompressible full Navier-Stokes equations written in generalized coordinates are solved directly without any turbulence model. All spatial derivatives except those of nonlinear terms are approximated by central difference for incompressible flow. The nonlinear terms are approximated by a third-order upwind scheme. This scheme has a numerical diffusion approximately expressed by fourth-order derivative.

Examples

1) Circular Cylinder

In order to capture the drag crisis, the flow was computed at Reynolds numbers 200000 and 400000. Figure 1 is the computed pressure contours which clearly show the difference of the flow patterns before and after the drag crisis. The number of grid points is 1000×100 . From this computation it can be said that the present method is suited to capture the characteristics of high Reynolds number flows.

2) Sphere

The unsteady flow fields around a sphere are presented in Figs. 2 and 3. Time development of pressure contour shows the mechanism of vortex shedding. Unstable flow patterns are recognized at the immediate leeward area of separation (Fig. 2). Various fluctuations of pressure distributions on the surface of a sphere manifest that instability generates wavy patterns over the circumference of the vortex rings.

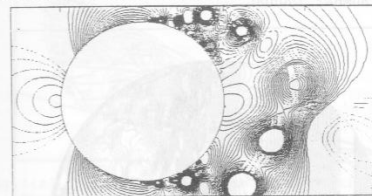
3) Slant-based body of revolution

Flow around a slant-based body of revolution with its axis aligned parallel to the uniform flow at Reynolds number $Re = 10^7$ is investigated. The dependence of the drag coefficient on the slant base angle is found to be in satisfactory quantitative agreement with the experimental data (Fig. 4). In particular, the drastic jump of the drag coefficient around the critical base angle, C_c , is captured successfully.

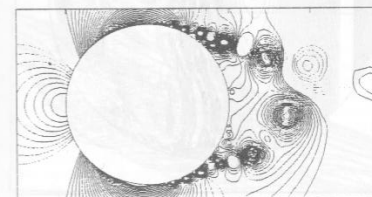
Extensive flow visualizations, using the computed results, have been made on two distinct separation patterns. When the base angle is smaller than C_c , the separation pattern is of the quasi-axisymmetric dead water type (Fig. 5). On the other hand, when the base angle is greater than C_c , the flow is characterized by a "U"-shaped vortex tube which originates from the base surface.

Conclusion

Owing to the development supercomputers, computational fluid dynamics has come to the stage where it can predict these detailed structure of high Reynolds number flows, not only in 2D but also in 3D by direct integration of the Navier-Stokes equations. These phenomena have not been able to be or have been very difficult to be observed by experiments.



(a) Reynolds number 200000.

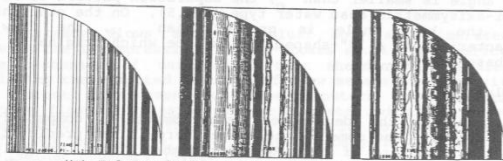


(b) Reynolds number 400000.

Fig.1 Pressure contours of a flow past a 2-D circular cylinder.



(a) On the body surface and center plane.



(b) Enlarged ones on the body surface.

Fig.2 Time development of pressure contours around a sphere. Reynolds number 100000.

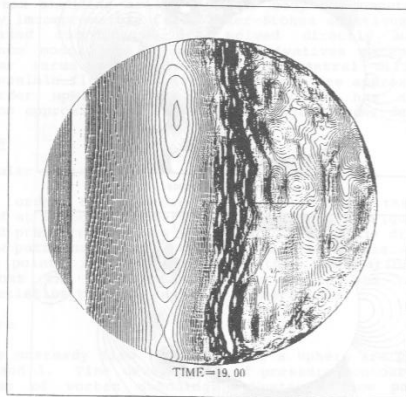


Fig.3 Instantaneous pressure distribution on the surface of a sphere at Reynolds number 100000.

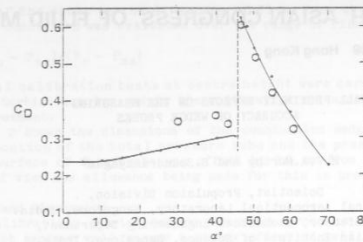


Fig.4 Drag coefficient variation with the slant base angle. The solid line indicates the experimental results by Morel, the present results are denoted by open circles.

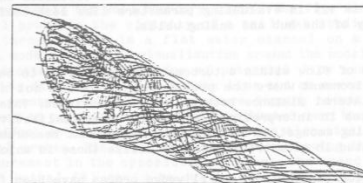


Fig.5(a) Instantaneous stream lines in the wake. The slant base angle is 40 degrees.

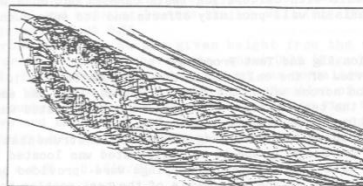


Fig.5(b) Instantaneous stream lines in the wake. The slant base angle is 50 degrees.